Center for Turbulence Research
Proceedings of the Summer Program 1992

Structure of turbulent non-premixed flames modeled with two-step chemistry

By J. H. Chen[1], S. Mahalingam[2], I. K. Puri[3] AND L. Vervisch[4]

Direct numerical simulations of turbulent diffusion flames modeled with finite-rate, two-step chemistry, $A + B \rightarrow I$, $A + I \rightarrow P$, were carried out. A detailed analysis of the turbulent flame structure reveals the complex nature of the penetration of various reactive species across two reaction zones in mixture fraction space. Due to this two-zone structure, these flames were found to be robust, resisting extinction over the parameter ranges investigated. As in single-step computations, mixture fraction dissipation rate and the mixture fraction were found to be statistically correlated. Simulations involving unequal molecular diffusivities suggest that the small scale mixing process and, hence, the turbulent flame structure is sensitive to the Schmidt number.

1. Introduction

The development of turbulent combustion models that accurately reflect key physical phenomena is essential for many engineering applications. Modern laser-based diagnostics applied to simplified laboratory flows are providing valuable data that is essential for any model development. However, since chemical reactions in flames proceed by a series of elementary steps, it is extremely difficult to isolate the role played by individual species and individual reaction steps on turbulent flame structure. Thus the task of studying the two-way coupling between turbulence and combustion becomes formidable. Recently, direct numerical simulations (DNS) of turbulent non-premixed flames with simplified chemistry have proven to be useful in studying various aspects of the problem.

DNS of turbulent diffusion flames including complex geometry and full chemistry is neither feasible with present-day computers, nor is it desirable since the objectives of DNS are usually to study specific aspects of the full problem. It is in this spirit that we studied the influence of turbulence on the structure of non-premixed flames in which chemistry is modeled through the following two- step mechanism:

$$A + B \rightarrow I \quad ; \quad A + I \rightarrow P. \tag{1}$$

The stoichiometric coefficients are chosen so that the global step is identical to the one step mechanism discussed by Chen *et al* (1992). The mechanism and the

1 Combustion Research Facility, Sandia National Laboratories, Livermore, CA
2 Center for Combustion Research, University of Colorado, Boulder, CO
3 Department of Mechanical Engineering, University of Illinois, Chicago, IL
4 Center for Turbulence Research

parameters were chosen to model step1 as a radical production step in which the intermediate I is produced followed by a radical consumption step in which the intermediate I is consumed to form the product P. Step2 proceeds with a small activation energy and a large enthalpy of reaction compared with step1. Usually, the intermediate radical species I diffuses at a faster rate compared with the other species. Only Fickian diffusion is modeled. Such reaction mechanisms have been studied using large activation energy (for both steps) asymptotics by Margolis and Matkowsky (1982). They point out that the case wherein the radical species concentration has a non-zero peak is typical of multi-step flames. The selected reaction mechanism may also be used to model practical flames (such as hydrocarbon oxidation) using global parameters. Altering the molecular diffusivity of the intermediate species can lead to modifications to flame structure and a change in flame temperature. This latter effect could be significant in accurately predicting thermal NOx formation in practical combustors (Law and Chung, 1984). Experimental measurements by Kerstein *et al* (1989) in nonreacting flows suggest that effects due to differential diffusion are not insignificant, and, hence, it is important to include them in models of chemically reacting flows. In reacting flows with significant heat release, these effects are likely to be amplified because of significant decrease in local Reynolds numbers due to an increase in kinematic viscosity with temperature.

The goal of this work is thus to obtain a good understanding of turbulent non-premixed flames modeled by a two-step mechanism, to identify the role of the intermediate species on flame structure, and to understand the significance of differential diffusion on flame structure.

2. Model problem

The problem studied is the interaction of turbulence with an initially unstrained laminar diffusion flame. Computations to date have been performed over a two-dimensional square domain with 129×129 equi-spaced grid points. A laminar diffusion flame in which species A and B are present on either side of the flame (located at approximately $x = 0$) is initialized. Non-reflecting boundary conditions in x and periodic boundary conditions in y are imposed. The full compressible form of the equations of continuity, Navier-Stokes, energy, and species are solved using higher-order finite differencing schemes. The code used was developed by Trouvé (1991) for 3D premixed flames and subsequently modified for non-premixed flames. The treatment of boundary conditions and the differencing scheme is based on the methodology of Poinsot and Lele (1991). Fluid viscosity varies with temperature according to a power law with an exponent of 0.76.

2.1 Governing equations and parameters

The governing equations and non-dimensionalization are discussed by Chen *et al* (1992). In this subsection, the evolution equations of various species and the parameters associated with the two-step chemistry model are discussed.

The generalized chemical scheme is given by:

$$\nu_{A_1} A + \nu_B B \rightarrow \nu_{I_1} I \quad ; \quad \nu_{A_2} A + \nu_{I_2} I \rightarrow \nu_P P, \tag{2}$$

where the ν's are the stoichiometric coefficients.

We define the following mass ratios:

$$r_{AB} = \frac{W_B \nu_B}{W_A \nu_{A_1}} \quad , \quad r_{AI_1} = \frac{W_I \nu_{I_1}}{W_A \nu_{A_1}} \quad , \quad r_{AI_2} = \frac{W_I \nu_{I_2}}{W_A \nu_{A_2}} \quad , \quad r_{AP} = \frac{W_P \nu_P}{W_A \nu_{A_2}}, \tag{3}$$

where W_A, W_B, W_I, and W_P are the molecular weights of species A, B, I, and P respectively.

In terms of mass, the overall reaction is given by

$$1A + rB \rightarrow (1+r)B \quad , \quad r = \frac{W_B \nu_B}{W_A \left[\nu_{A_1} + \nu_{A_2} \frac{\nu_{I_1}}{\nu_{I_2}}\right]}. \tag{4}$$

Let q_1 and q_2 be the energy released per unit mass of species A consumed in step1 and step2 respectively, and let $\delta = q_2/q_1$. Then from the definition of the adiabatic flame temperature, one can show that the following equality, expressing global energy conservation, has to be satisfied:

$$q_1 \left[\epsilon + \delta(1-\epsilon)\right] = \frac{1}{Y_{A,0}} \left[1 + \phi\right] c_p (T_f - T_0) \quad , \quad \epsilon = \frac{\nu_{A_1}}{\nu_{A_1} + \nu_{A_2} \frac{\nu_{I_1}}{\nu_{I_2}}}, \tag{5}$$

where T_f is the adiabatic flame temperature, $Y_{A,0}$ is the mass fraction of species A in the unmixed A stream, c_p is the specific heat, T_0 is the temperature of the unmixed A and B streams, and ϕ is the overall equivalence ratio defined as:

$$\phi = r \frac{Y_{A,0}}{Y_{B,0}}, \tag{6}$$

where $Y_{B,0}$ is the mass fraction of species B in the unmixed B stream. Continuity and Navier–Stokes equations are given in Chen *et al* (1992) and are not repeated here. The energy and species equations are:

$$\frac{\partial \rho E}{\partial t} + \frac{\partial (\rho E + p) u_i}{\partial x_i} = \frac{\partial (u_j \tau_{ij})}{\partial x_i} + \frac{\partial}{\partial x_i}\left(\lambda \frac{\partial T}{\partial x_i}\right) + q_1 \dot{w}_{A_1} + q_2 \dot{w}_{A_2}, \tag{7}$$

$$\frac{\partial \rho Y_A}{\partial t} + \frac{\partial \rho Y_A u_i}{\partial x_i} = \frac{\partial}{\partial x_i}\left(\rho \mathcal{D}_A \frac{\partial Y_A}{\partial x_i}\right) - \dot{w}_{A_1} - \dot{w}_{A_2}, \tag{8}$$

$$\frac{\partial \rho Y_B}{\partial t} + \frac{\partial \rho Y_B u_i}{\partial x_i} = \frac{\partial}{\partial x_i}\left(\rho \mathcal{D}_B \frac{\partial Y_B}{\partial x_i}\right) - r_{AB} \dot{w}_{A_1}, \tag{9}$$

$$\frac{\partial \rho Y_I}{\partial t} + \frac{\partial \rho Y_I u_i}{\partial x_i} = \frac{\partial}{\partial x_i}\left(\rho \mathcal{D}_I \frac{\partial Y_I}{\partial x_i}\right) + r_{AI_1} \dot{w}_{A_1} - r_{AI_2} \dot{w}_{A_2}, \tag{10}$$

$$\frac{\partial \rho Y_P}{\partial t} + \frac{\partial \rho Y_P u_i}{\partial x_i} = \frac{\partial}{\partial x_i}\left(\rho \mathcal{D}_P \frac{\partial Y_P}{\partial x_i}\right) + r_{AP} \dot{w}_{A_2}, \tag{11}$$

where

$$\rho E = \frac{\rho u_k u_k}{2} + \frac{p}{\gamma - 1}. \tag{12}$$

In the above equations, ρ denotes the fluid density, E denotes the total (internal plus kinetic) energy per unit mass, and γ is the specific heat ratio taken to be 1.4. The thermal conductivity λ and the molecular diffusivities $\mathcal{D}_A, \mathcal{D}_B, \mathcal{D}_I$, and $\mathcal{D}_P$ are related to the dynamic viscosity μ through the Prandtl and species Schmidt numbers. The other symbols have the usual meaning as in the standard literature. The reaction rate terms $\dot{w}_{A_1}$ and $\dot{w}_{A_2}$ are given by the Arrhenius expressions:

$$\dot{w}_{A_1} = B_1 \rho Y_A \rho Y_B \exp\left(-\frac{T_{a_1}}{T}\right), \quad \text{and} \quad \dot{w}_{A_2} = B_2 \rho Y_A \rho Y_I \exp\left(-\frac{T_{a_2}}{T}\right), \tag{13}$$

or alternatively in the form:

$$\dot{w}_{A_1} = \mathbf{B}_1 \rho Y_A \rho Y_B \exp\left(\frac{-\beta_1(1-\tau)}{1-\alpha(1-\tau)}\right), \tag{14}$$

and

$$\dot{w}_{A_2} = \mathbf{B}_2 \rho Y_A \rho Y_I \exp\left(\frac{-\beta_2(1-\tau)}{1-\alpha(1-\tau)}\right), \tag{15}$$

where T_{a_1} and T_{a_2} are the activation temperatures associated with step1 and step2, τ is a nondimensional temperature defined as $\tau = (T - T_0)/(T_f - T_0)$ as given by Williams (1985), $\mathbf{B}_1 = B_1 \exp(-\beta_1/\alpha)$ and $\mathbf{B}_2 = B_2 \exp(-\beta_2/\alpha)$ are the pre-exponential factors, and α is a temperature factor defined as $\alpha = (T_f - T_0)/T_f$.

In the simulations reported here, the following values were chosen for the stoichiometric coefficients: $\nu_{A_1} = \nu_{A_2} = 1/2$, $\nu_B = \nu_{I_1} = \nu_{I_2} = \nu_P = 1$, so that the overall scheme corresponds to the one-step model used by Chen *et al* (1992). Values for other constants are: $\alpha = 0.8$, $\beta_1 = 8$, $\beta_2 = 2$, $\delta = 5$, consistent with the discussion in Section 1. The value of the Prandtl number is unity. The Schmidt numbers are $Sc_A = Sc_B = Sc_P = 1$. The Schmidt number of the intermediate species $Sc_I = 1$ unless otherwise noted.

2.2 Initial conditions and turbulence field

The generation of initial conditions corresponding to profiles associated with a one-dimensional, unstrained laminar diffusion flame was achieved by the following procedure: the flowfield is initialized with the solution to the one-step chemistry problem discussed by Chen *et al* (1992). The second reaction is turned "off" by setting $B_2 = 0$, and the product profile for the one-step model is used as the profile for species I. The equations are time-advanced, and, simultaneously, the pre-exponential coefficient B_2 is increased until the desired value is reached. Care is taken to ensure that the flame does not extinguish during this process. Once the pressure waves exit the domain, the flowfield is saved (after any required rescaling), and, from this point forward, the turbulence is allowed to interact with the flame.

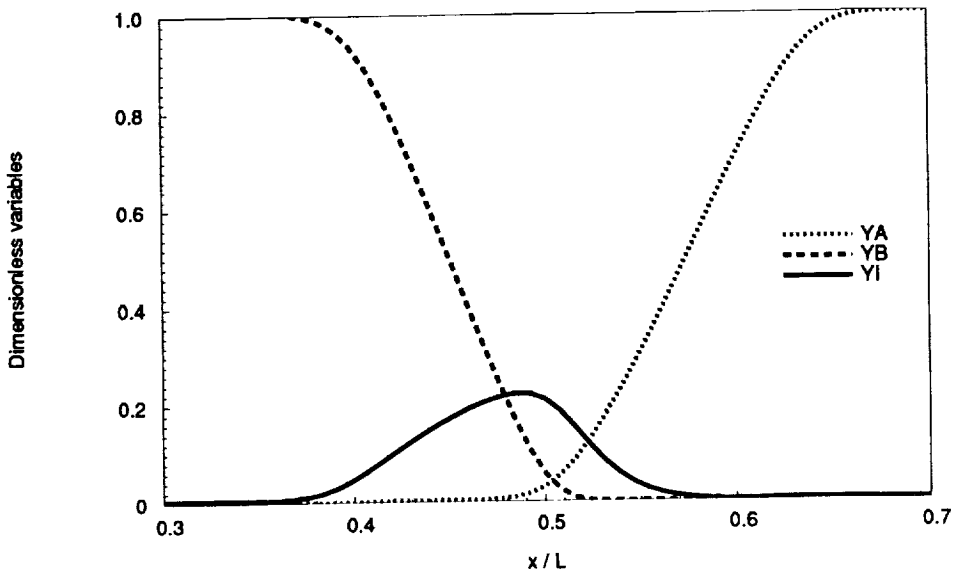

FIGURE 1. Species concentration profiles across the initial 1D laminar flame for a representative condition ($Da = 1$).

For details on the turbulence characteristics and definition of the global Damköhler number, Chen *et al* (1992) may be consulted. A plot of the species profiles of the laminar flame is presented in Figure 1. It is clear that the concentration of the intermediate is significant. Its peak value is a measure of the extent of physical separation between reaction zones associated with the production (step1) and consumption (step2) of the intermediate species.

3. Results and discussion

A quantity that is often used in descriptions of non-premixed flames is the mixture fraction, defined for our choice of stoichiometric coefficients, molecular weight,s and unmixed stream concentrations as:

$$Z = \frac{2Y_A - Y_I - 2Y_B + 2}{4}, \tag{16}$$

such that in the unmixed A stream, $Z = 1$, and in the unmixed B stream, $Z = 0$. When all the molecular diffusion coefficients are equal, Z is a conserved scalar. In the limit of infinitely fast chemistry, at the flame $Y_A = Y_B = Y_I = 0$, giving $Z_{c1} = 1/2$, whereas if the second step is relatively slow compared to the first step, at the flame $Y_A = Y_B = 0$, $Y_I = 1$, giving $Z_{c2} = 1/4$. Thus these two limits of Z identify the locations of the reaction zones under these limiting cases. Finite rate chemistry will tend to cause a deviation from these two stoichiometric surface locations. Note that Z is not a conserved scalar when the diffusivities of the various

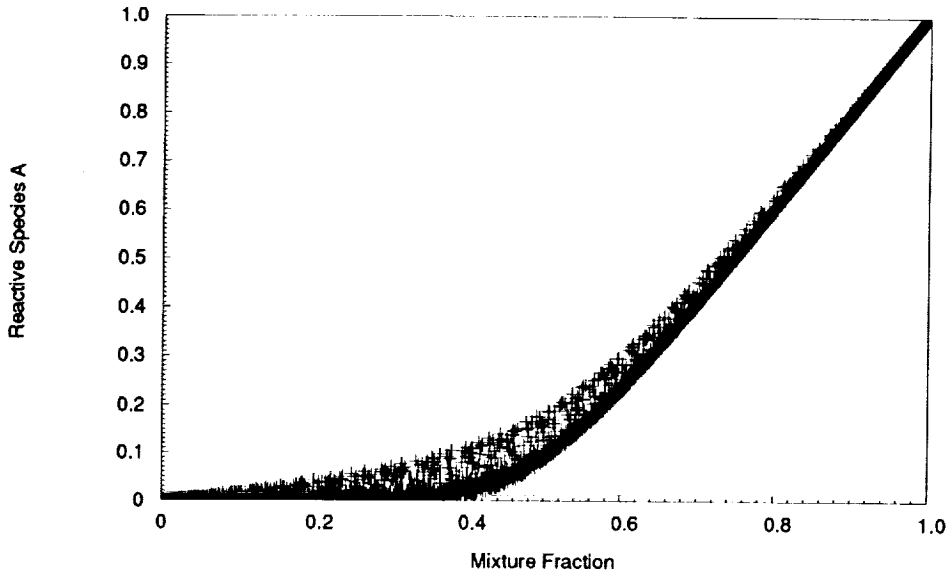

FIGURE 2(A). Distribution of species A mass fraction Y_A, versus mixture fraction Z ($Da = 1$).

species are not equal. In Figure 2(a), the mass fraction Y_A is plotted as a function of Z. It is clear that most of the data points lie close to the equilibrium line, represented by the lower boundary of the data points. The penetration of species A into the B regime is due to finite rate kinetics. The scatter in these data points is due to unsteady effects associated with the turbulence field. The variations of Y_B and Y_I and the reduced temperature τ are shown in Figures 2(b)-(d). These results are consistent with Figure 2(a). It is apparent from Figure 2(d) that no significant drop in temperature is seen, suggesting that extinction is not seen for the conditions of the present simulation.

Reaction rate profiles associated with steps1 and 2, respectively, are presented in Figures 3(a)-(b). Several features may be readily observed. It is clear that reaction rates for steps 1 and 2 peak for $Z \approx 0.45$ and $Z \approx 0.58$, respectively. Since the mass fraction of species I is significant where reaction 1 occurs, it is apparent from the definition of Z that the shift would be towards lower values of Z. Reaction 2 occurs on the A side of the flame, where A is in excess, thus shifting the peak towards larger values of Z. For the parameters chosen, we have two reaction zones that are not completely segregated in mixture fraction (and physical) space. It is clear from these plots and the plot of reduced temperature (Figure 2(d)) that *no extinction* has occurred in either step. This is a significant observation since the global Damköhler number is comparable to the case for single–step chemistry for which extinction was observed (see Chen *et al*, 1992). An increase in the number of radical–like species and segregation of reaction zones apparently makes the flame

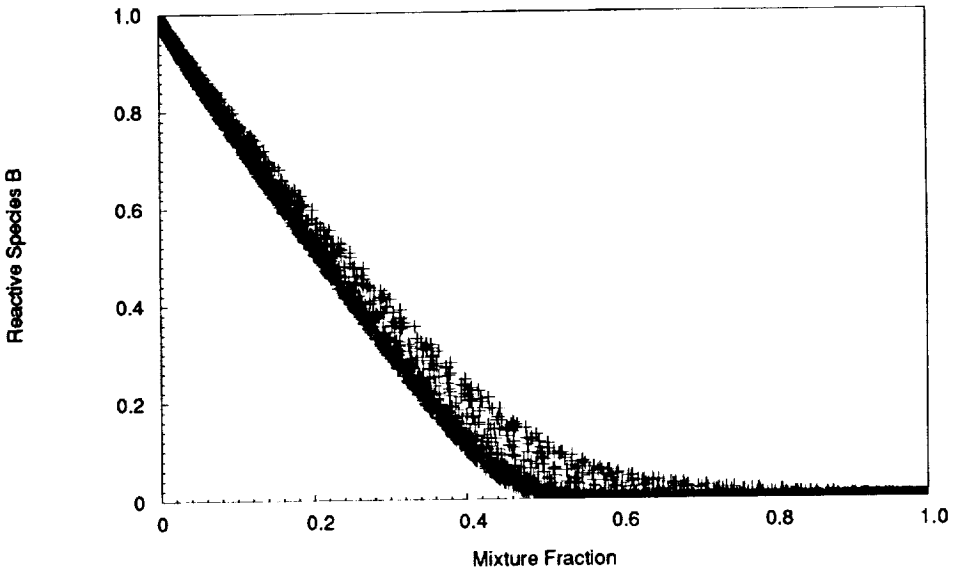

FIGURE 2(B). Distribution of species B mass fraction Y_B, versus mixture fraction ($Da = 1$).

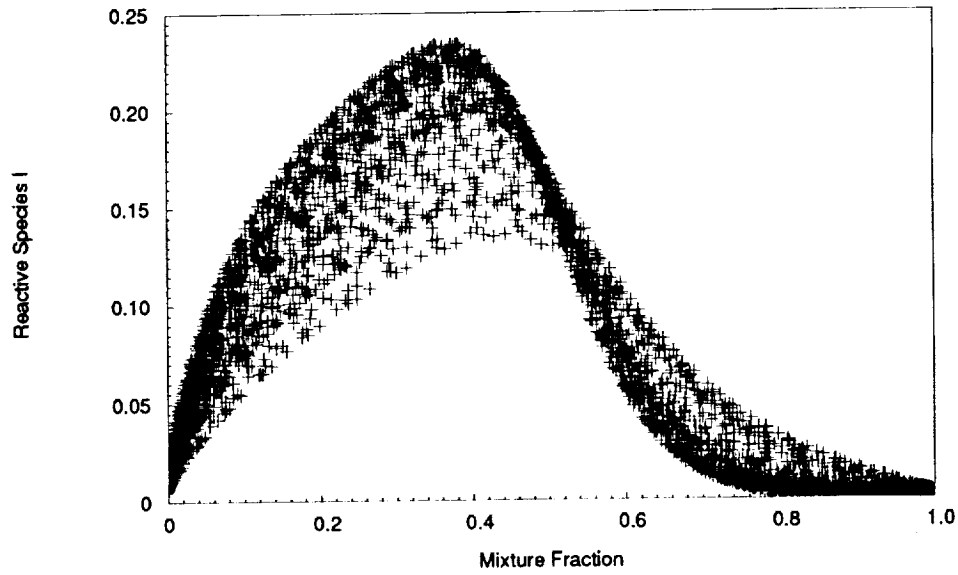

FIGURE 2(C). Distribution of intermediate species I mass fraction Y_I, versus mixture fraction ($Da = 1$).

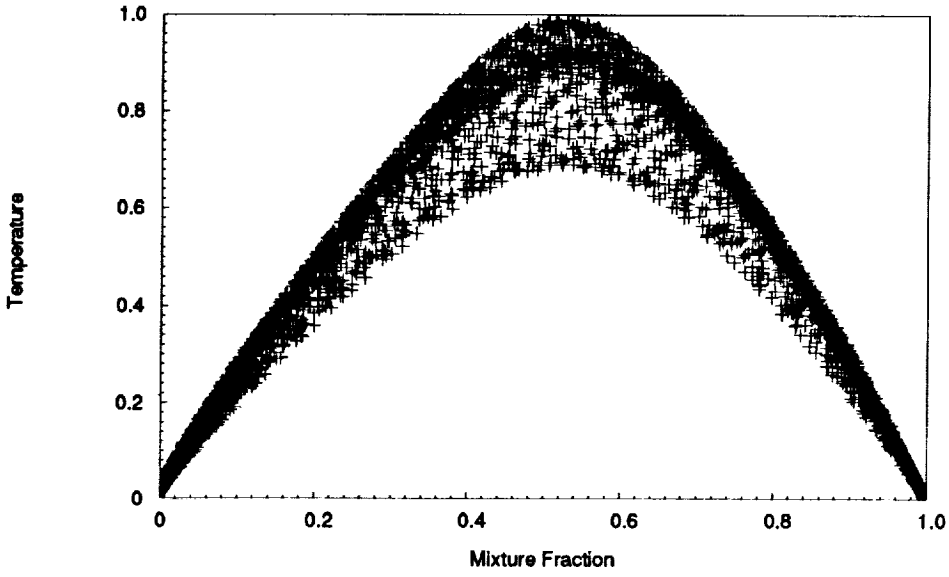

FIGURE 2(D). Distribution of reduced temperature τ versus mixture fraction ($Da = 1$).

less sensitive to extinction either by strain or flame shortening.

A quantity that may be used to characterize reaction–diffusion zones is the scalar dissipation rate of the appropriate scalar, defined for species A as:

$$\chi_A = 2\mathcal{D}_A \nabla Y_A \cdot \nabla Y_A \tag{17}$$

In Figures 4(a)-(c), the scalar dissipation rates of scalars A, B, and the intermediate species I are plotted as functions of mixture fraction. Results for species A are very similar to that for species A in the single step case (compare with Figure 2(b) in Chen *et al*, 1992), with the peak occurring at a mixture fraction of approximately 0.7. Note, however, that there are no data points corresponding to frozen flow in the present case. This is consistent with the fact that no extinction was observed for the conditions simulated. Penetration of species A into the B side is apparent, but this is solely due to finite–rate kinetics. The scatter in the data points is due to unsteady effects. Results for species B complement those for A. Results for species I are interesting. If the second reaction were suppressed, it is clear that one would see a minimum in χ_I for $Z = 0.5$, with two symmetric peaks on either side, corresponding to locations where the molecular diffusion of species I would be highest. Note that since I is consumed by A in step2, the peak on the A side is enhanced, relative to the peak on the B side, with the minimum shifted to approximately $Z = 0.4$. This location corresponds to generation of species I by step 1.

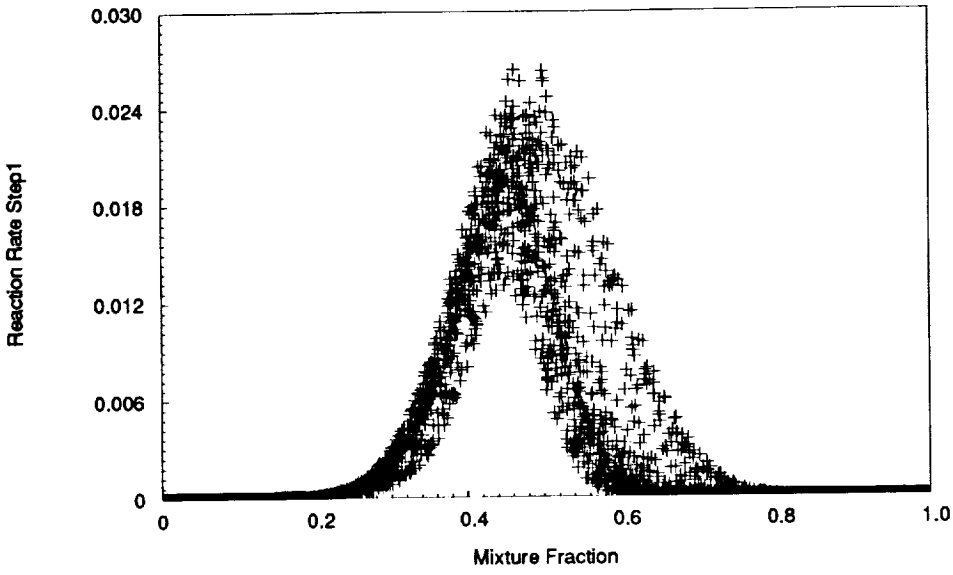

FIGURE 3(A). Distribution of reaction rate for step 1 versus mixture fraction ($Da = 1$).

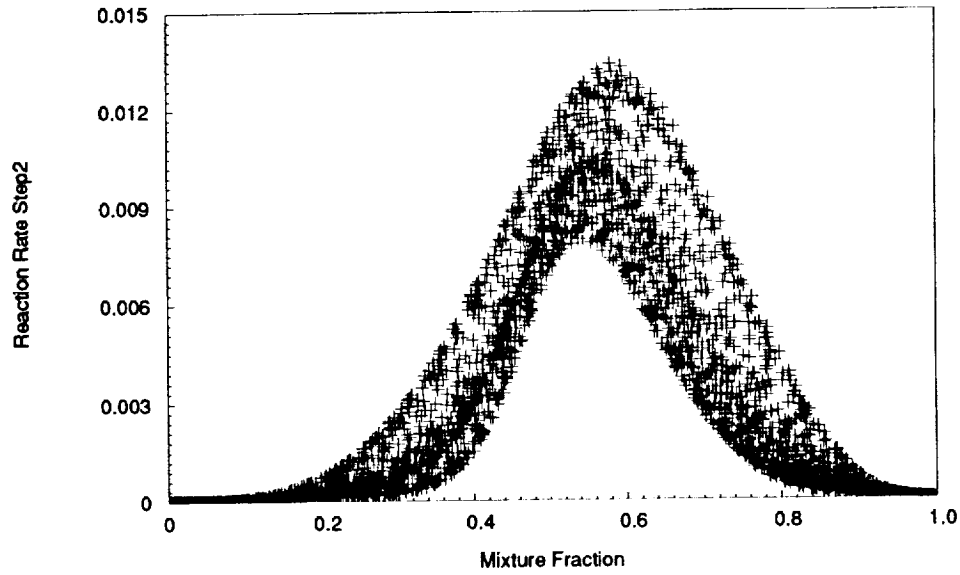

FIGURE 3(B). Distribution of reaction rate for step 2 versus mixture fraction ($Da = 1$).

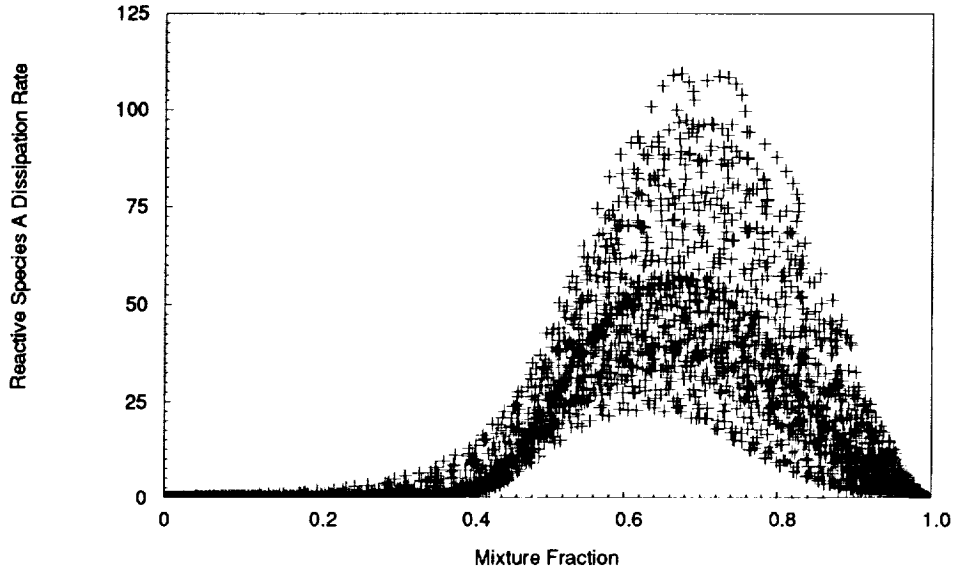

FIGURE 4(A). Distribution of dissipation rate of species A versus mixture fraction ($Da = 1$).

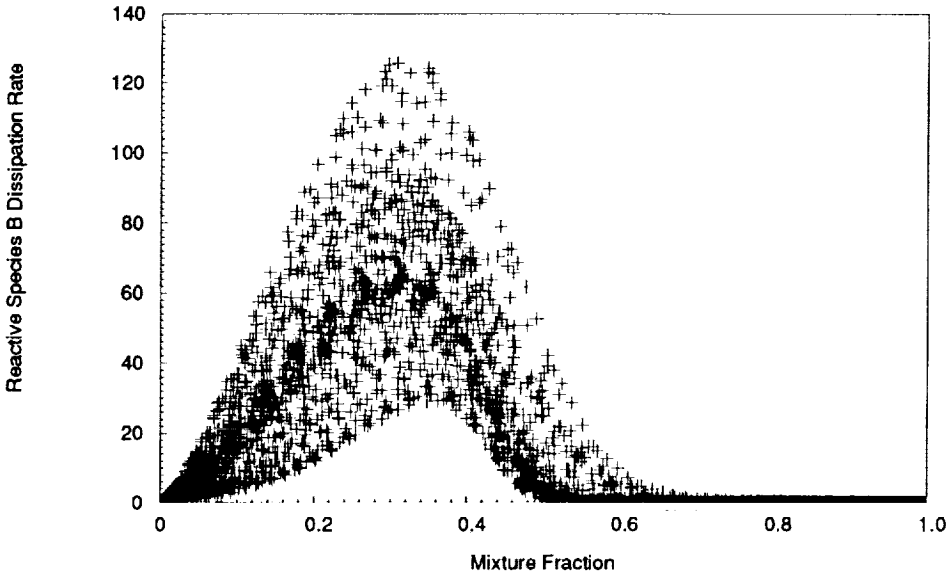

FIGURE 4(B). Distribution of dissipation rate of species B versus mixture fraction ($Da = 1$).

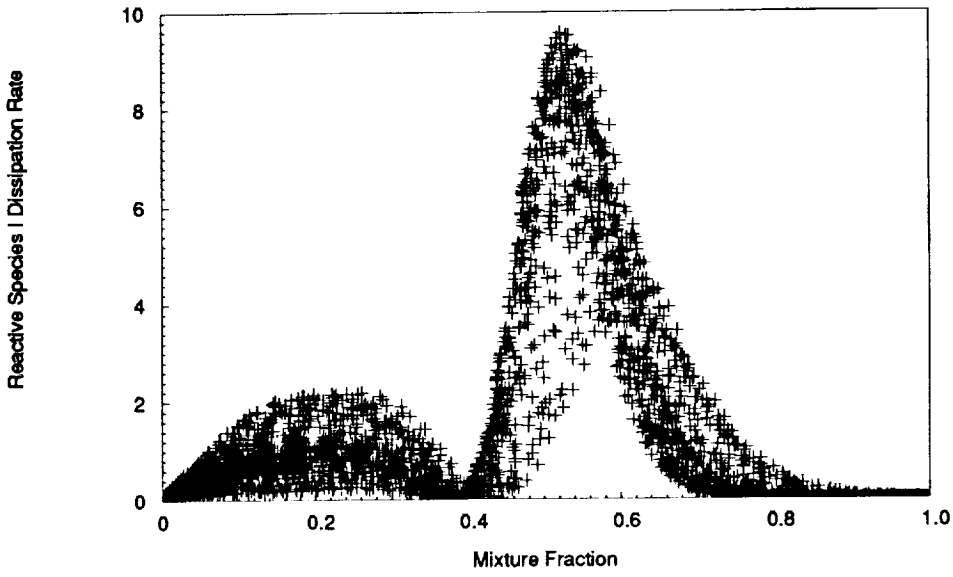

FIGURE 4(c). Distribution of dissipation rate of intermediate species I versus mixture fraction ($Da = 1$).

In Figure 5(a), the distribution of the scalar dissipation rate of the intermediate as a function of the mixture fraction for $Sc_I = 0.5$ is shown. It is clear that the rapidly diffusing intermediate species penetrates further into the A side (compare with Figure 4(c)). Instantaneous contour plots of χ_I in physical space for $Sc_I = 1$ and $Sc_I = 0.5$, shown in Figures 5(b)-(c), reveals that the dissipation zone is larger when the species diffusion coefficient is larger (ie., Sc_I lower). This result suggests that small scale mixing is sensitive to the molecular diffusion coefficient of the intermediate species even though turbulent diffusion is the more active process. It is clear that three dimensional results need to be examined before one can draw definitive conclusions.

In Figure 6, the mixture fraction dissipation rate χ defined as:

$$\chi = 2\mathcal{D}\nabla Z \cdot \nabla Z, \tag{18}$$

is plotted as a function of mixture fraction.

This picture is qualitatively similar to the results for single step chemistry presented by Chen *et al* (1992), with the exception that no extinction is observed in the present case. It is clear that a correlation exists between χ and Z contrary to the assumptions made in laminar flamelet theories (Peters, 1986, Warnatz and Rogg, 1986).

4. Conclusions

From the first study of non-premixed flames modeled by a two-step reaction

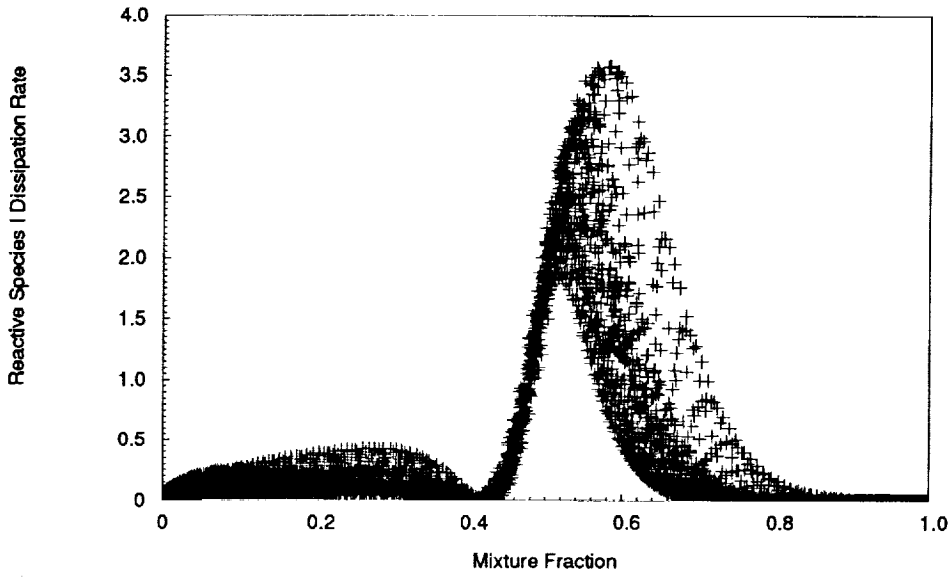

FIGURE 5(A). Distribution of dissipation rate of intermediate species I versus mixture fraction ($Sc_I = 0.5, Da = 1$).

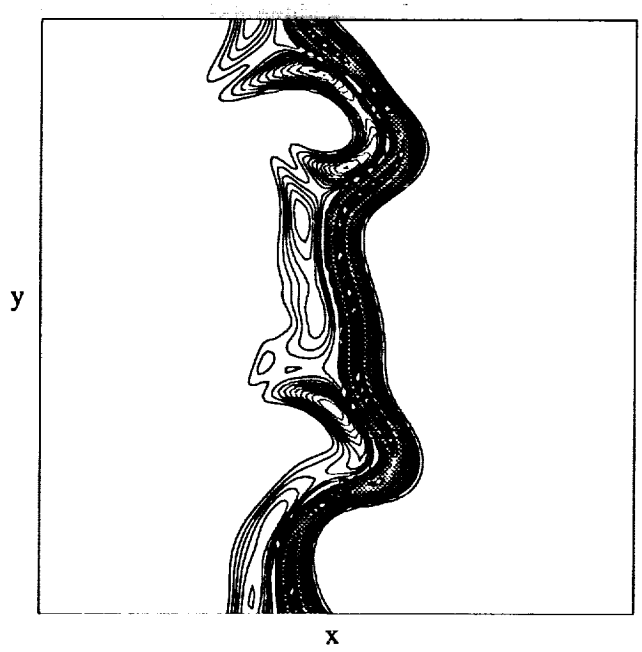

FIGURE 5(B). Intermediate species dissipation rate contours ($Sc_I = 1.0, Da = 1$).

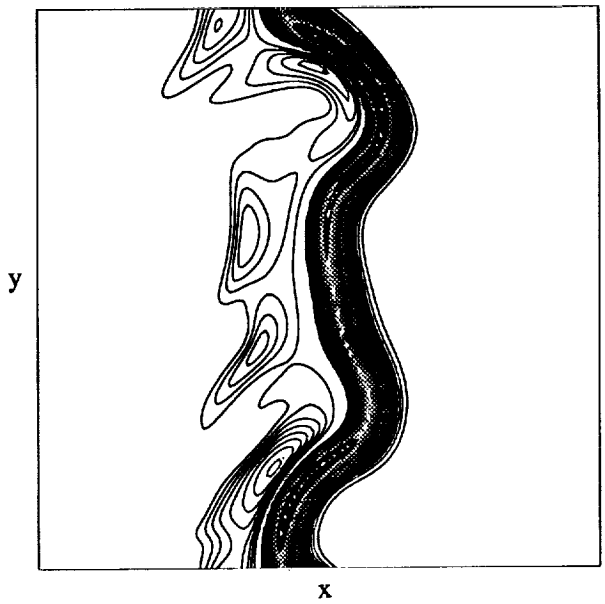

FIGURE 5(c). Intermediate species dissipation rate contours ($Sc_I = 0.5, Da = 1$).

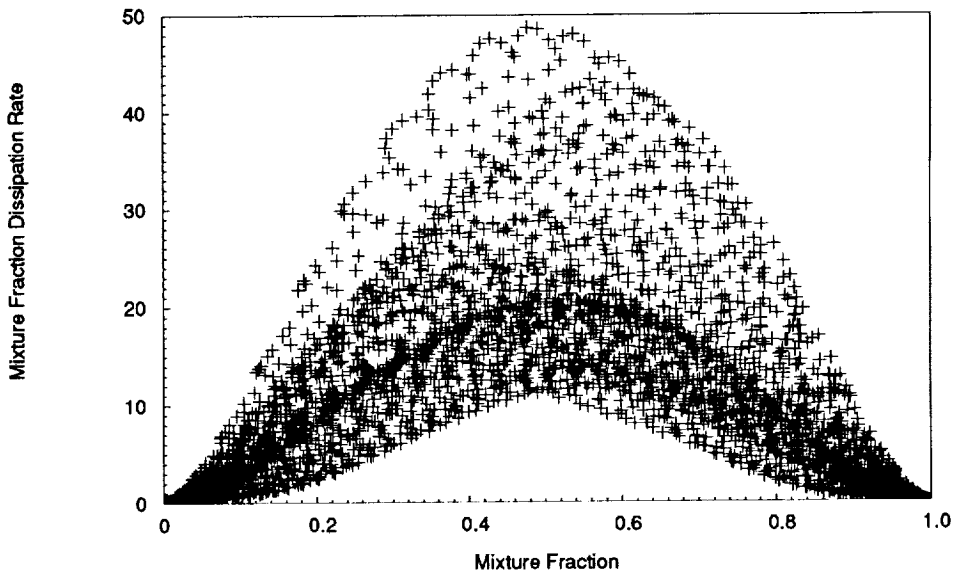

FIGURE 6. Distribution of the scalar dissipation rate χ with respect to the mixture fraction ($Da = 1$).

mechanism in a compressible, turbulent flow, two–dimensional databases were generated. Finite values of the intermediate species mass fraction arise as a result of a slight segregation of the reaction zones associated with the two steps. A consequence of the segregated reaction zones is that the flame is less susceptible to extinction compared to flames modeled with a single–step, having an equivalent overall reaction step. It was demonstrated that the assumption of statistical independence between the mixture fraction and its dissipation rate is a poor one, invalidating an important assumption made in flamelet models. It is expected that these results would hold for three–dimensional simulations currently in progress. Preliminary results from simulations in which the intermediate species diffuses at twice the rate compared to the other species suggest that the small scale mixing process and, hence, the turbulent flame structure is significantly influenced. Further examinations of the flame structure and flame response to turbulence are being carried out.

Acknowledgements

The authors have benefited from discussions with the other members of the combustion group during the 1992 CTR summer program, in particular with Dr. Arnaud Trouvé and Dr. Thierry Poinsot. We also thank Prof. Forman Williams and Prof. Stephen Pope for their helpful comments and suggestions. J. H. Chen has been supported for this work by the department of Energy's Office of Basic Energy Sciences, Division of Chemical Sciences.

REFERENCES

KERSTEIN, A., DIBBLE R., LONG, M. 1989 Proceedings of the Seventh Turbulent Shear Flows Symposium, Stanford University, Stanford.

LAW, C. K., CHUNG, S. H. 1982 Steady state diffusion flame structure with Lewis number variations. *Combust. Sci. and Tech.* **29,** 129–145.

MARGOLIS, S. B., MATKOWSKY, B. J. 1982 Steady and pulsating modes of sequential flame propagation. *Combust. Sci. and Tech.* **27,** 193–213.

PETERS, N. 1986 Laminar flamelet concepts in turbulent combustion. *Twenty–First Symposium (International) on Combustion.* 1231–1250. The Combustion Institute.

POINSOT, T., LELE, S. 1991 Boundary conditions for direct simulations of compressible viscous flows. *J. Comput. Phys.* **101,** No 1, July 92

TROUVE, A. 1991 Simulation of flame-turbulence interaction in premixed combustion. *Annual Research Briefs, CTR, Stanford U.*

WARNATZ, J., ROGG, B. 1986 Turbulent non-premixed combustion in partially premixed flamelets detailed chemistry. *Twenty–First Symposium (International) on Combustion.* 1533-1541. The Combustion Institute.

WILLIAMS, F. A. 1985 Combustion Theory, Benjamin/Cummings Publishing Company